Potential application of a triaxial three-dimensional fabric (3-DF) as an implant

Y. Shikinami*, H. Kawarada

Takiron Co., Ltd, 405 Nagano, Yasutomi-cho, Shisou-gun, Hyogo-ken, 671-24, Japan

Abstract

Various three-dimensional fabrics (3-DFs) woven with a triaxial three-dimensional (3A-3D) structure in which the warps, wefts and vertical fibres are three-dimensionally orientated with orthogonal, off-angle, cylindrical or complex fibre alignments using a single long fibre, which may be one of several kinds of fibres, have been developed. The physical strengths and behaviour of these fabrics under different external forces were measured for such stress–strain relationships as compressive, tensile and cyclic bending, compressing torsional and compressive tensile systems to evaluate the effect of the continuous loading caused by living body movements over a long period of time. The 3-DFs led to downward convex 'J'-shaped curves in stress–strain profiles, because they were markedly flexible at low strain levels, but became rigid as strain increased. In this behaviour they reflected the behaviour of natural cartilage rather than that of conventional artificial biomaterials. There were also some 3-DFs that showed hysteresis loss curves with quite similar mechanical strengths and behaviour to natural intervertebral discs with regard to the compressive-tensile cyclic stress and showed little variation from the first 'J'-shaped hysteresis profile even after 100, 000 deformation cycles. Accordingly, it has been shown that, without a doubt, 3-DFs can be effective implants possessing both design and mechanical biocompatibilities as well as the durability necessary for long-term implantation in the living body. The surface of bioinert linear low-density polyethylene coating on multifilaments of ultra-high molecular weight polyethylene, a constructional fibre of 3A-3D weaving, was modified by treatment with corona-discharge and spray-coating of unsintered hydroxyapatite powder to impart chemical (surface) compatibility and biological activity, respectively. Since the modified surface of the 3-DF was ascertained to have affinity and activity with simulated body fluid, an orthogonal 3-DF block was implanted in the tibia of a rabbit. Sufficient surrounding tissues entering into the textural space of the 3-DF could be observed at 4 weeks after implantation and the load necessary to break the block away from the bone reached a high value at 8 weeks. These results decisively showed that the 3-DFs could also acquire chemical (surface) and biological biocompatibilities and bonding capacity with bone and soft tissues through modification of the surface of the constructional fibre. The 3-DFs have definite potential in such applications as novel and effective artificial articular cartilages, intervertebral discs, menisci and materials for osteosynthesis and prosthesis, and the like. © 1998 Elsevier Science Ltd. All rights reserved

Keywords: Fibrous implants; Three-dimensional fabrics; Bulk and surface biocompatibility; Artificial cartilages; Artificial intervertebral disc; Biomechanic

1. Introduction

This article relates to:

(1) the creation of novel and effective biomaterials constructed by cubic three-dimensional fabrics (3-DFs) having triaxial (3A) fibre alignment, and

(2) the evaluation of their potential application as artificial bones, cartilages, menisci and finger joints, bone fillers, materials for osteosynthesis and prosthesis, and other such applications

and as such these biomaterials exhibit both interfacial (biological) and bulk (mechanical) biocompatibilities including the ability to bind to the living body.

All biological tissues having, for example, a cubic shape, are always produced in three dimensions and are never orientated in only two dimensions. Their physical strengths and behaviour in all directions (length, width and height) also naturally vary. Almost all artificial biomaterials to date have been developed with the aim of

---

*Corresponding author. Tel.: 0081 790 66 2411; fax: 0081 790 66 3717.

having higher apparent strength than those of the living body with the reasoning that physical durability and breaking resistance would increase with increasing mechanical strength. This same high strength in three dimensions causes trouble in the long-term due to ill-matching between the implant and the adjacent tissue. This research proposes a method to solve these problems.

The three-dimensional fabric (3-DF) of this article can be defined as having a cubic structure made by three-dimensional weaving or knitting, whereby a continuous long filament fibre is orientated in both in-plane and out-of-plane directions, that is, in the direction passing through the thickness of the fabric. A three-dimensional woven composite (3-DC) in which a heat resistant and high strength material is filled as a matrix among the textural space of 3-DF has been put into various trials over the past 30 years or so, mainly with the aim of developing industrial and aircraft materials, which demand high strength in three dimensions and must not cause strain under high temperatures [1–7]. The 3-DC is a specific composite material comprising carbon or ceramic fibres and, in most cases, matrices thereof. It cannot be used as a biomaterial as there are concerns about it breaking into fragments, because it is so rigid yet fragile.

There have been several trials and descriptions concerned with the potential applications of 3-DC or 3-DF as new fibre structures suitable for reinforced load-bearing implants such as in osteosynthesis [8–15] or scaffold devices [16–19]. Actually, there is an artificial blood vessel made of polyester fibres in a tubular form having a thin wall thickness which is produced by triaxial weaving and exhibits three-dimensional expansion [20]. However, this vessel is a fabric product in which threads in the directions of three axes are crossed at an angle of 60° in the same plane and which was developed with the aim of improving the anisotropy (bias) of the plane fabric; therefore, it can be classified as a cylindrical fabric corresponding to a triaxial-two-dimensional (3A-2D) textural type.

Alternatively, an artificial ligament in the shape of a cord has been made of polyester or polypropylene filaments, which are woven as a monoaxial three-dimensional (1A-3D) braid (3-DB: three-dimensional braid) [21–26]. However, to date a practical cubic 3-DF especially of 3A-3D, applicable to clinical use as an implant, had not been found.

3-DF may be a successful implant material, because it can be made with various structures having clear cubic shapes (designs), sizes and volumes, and it can offer sufficient strength and dynamic mechanical behaviour to stand up to living body movements. Among the possible multiaxial (mA: $m \geqslant 3$, positive integers) fibre alignments, only triaxial (3A) alignments were chosen for the 3-DF of this article. Namely, for implants, this article limited the 3-DFs to triaxial three-dimensional (3A-3D) fabrics. An indispensable property for biomaterials, biocompatibility

can generally be divided into two constituents [27–31],

   (A) an unstimulative property due to insignificant foreign body reaction, and

   (B) tissue connectivity.

(A) can be further divided into two compatibilities:

   (i) the bulk (mechanical) property, and

   (ii) the surface (biological) property.

Surface modification of polymers for medical applications has been thoroughly investigated to improve the interfacial biocompatibility [32]. Implants compatible with living tissue and which possess mechanical and structural consistencies, such as absolute strength, compliance, shape (design) and long-term durability, etc., have seldom been accomplished. To date, biomaterials having both these types of biocompatibility have not been very successful. This paper proposes a biomaterial as an aforementioned implant material achieving these two biocompatibilities.

2. Experimental

2.1. Manufacture of 3-DF cubic structures

The constructional mode of woven fabrics can generally be classified by either the dimensional number relating to the geometric shape of the body or the axial number expressing the azimuth number of the fibre alignment. Therefore, the fibre arrangement in which the warps, wefts and vertical fibres are three-dimensionally orientated can be classified as a triaxial three-dimensional (3A-3D) weaving pattern. Table 1 shows the classification of 3-DFs (FABRICUBE™) woven by the 3A-3D combinations used in these experiments. These 3-DF cubic structures were produced by the methods given in the following.

For all the samples except sample nos 8 and 9, in Table 1, a fibre with an average diameter of 400 μm was prepared by melting a linear low density polyethylene (LLDPE—Idemitsu Polyethylene L; $M_W = 84{,}000$; manufactured by Idemitsu Petrochemical Co., Ltd) at 120°C and using the extruding process to coat it on the surface of an ultra-high molecular weight polyethylene fibre (UHMWPE—Techmiron®; manufactured by Mitsui Petrochemical Co., Ltd) of 500 denier (50 filaments) and an average thickness of 85 μm (Fibre A). By this treatment, it was possible to avoid the loosening of the fibre into individual filaments, even after loading with a shear force for long periods of time.

Fibre A was treated by a hand operation practice machine using triaxial weaving technology as described by Dow [33] and Tranfield, and Hirokawa [34] to produce 3A-3D structures. As shown in Table 1, these structures included several sizes of various block-, near-net- or pseudo-cylindrical-shaped fabrics with orthogonal or off-angle fibre alignments or a combination of

Table 1
Classification of 3-DFs (FABRICUBE™) woven by 3A–3D combinations

Sample No.		1	2	3	4	5	6	7	8	9	10	11	12	13
Fibre material		LLDPE/UHMWPE							PVA	Polyester fibre	LLDPE/UHMWPE			A B
Classification of 3-DF construction	Fibre alignment	A	B	A	B	A	B	B	A	A	C	A	B	F
	Shape	D	D	D	D	E	E	E	E	E	E	D	F	
Arrangement (number)														
warp × layer		15×69	22×100	21×69	41×69	24×75	23×140	17×140	20×31	24×41	19×54	6×15	9×30	—
weft × layer		15×69	22×100	75×69	41×69	35×75	23×140	17×140	30×31	35×41	18×54	6×15	9×30	—
vertical fibre × folding		321×4	144×4	1572×4	780×4	730×4	138×4	119×4	144×4	730×4	399×4	49×4	34×2	174×4
x y plane		19	14	10	9	9	10	10	6	8	7	4	5	—
pitch of x y plane (m/m)		1.4	2.12	1.5	2.0	1.4	2.12	1.73	2.12	2.5	1.4	1.4	1.4	1.6
Alignment ratio (x:y:z)		1:1:1	3:3:2 (v:w:z)	1:1:1	3:3:1 (v:w:z)	1:1:1	4:4:1 (v:w:z)	5:5:1 (v:w:z)	3:3:2	1:1:1	6:6:1 (v:w:z)	3:3:2 (v:w:z)	4:4:1	—

Appearance (size; mm)

Loading and axial direction →

Fibre alignment → ---- [a]

No.1 (x,y, 90°) (24.3×24.3×24.0)
No.2 (v,w, ±45°) (25.5×25.6×24.7)
No.3 (x,y, 90°) (101.5×29.0×12.5)
No.4 (v,w, ±45°) (101.2×28.7×13.2)
No.5 (x,y, 90°) (50.0×35.0×13.3)
No.6 (v,w, ±45°) (47.0×36.1×15.2)
No.7 (v,w, ±30°) (45.7×34.8×15.8)
No.8 (x,y, 90°) (44.7×30.4×8.4)
No.9 (x,y, 90°) (50.7×36.2×11.2)
No.10 (v,w, ±45°) (46.8×39.2×16.8)
No.11 (x,y, 90°) (9.8×9.0×3.2)
No.12 (v,w, ±45°) (31.9×11.4×3.8)
No.13 (x,y, 90°) (33.2×23.4×6.0)

LLDPE/UHMWPE: LDPE coated UHMWPE filaments.
A: orthogonal, B: off-angle, C: pseudo-cylindrical, D: block, E: near-net, F: complex.
[a] Loading and axial directions are coincident with fibre alignments in nos. 1, 3, 5, 8, 9 and 11.

orthogonal and off-angle fibre alignments in different parts of the fabric and these fabrics consisted of a number of fibres in the x-, y- and z-axes and their respective multilayers with some alignment ratios (weight ratio or fibre length ratio) in three dimensions. A semi-elliptically shaped near-net 3-DF, sample no. 8 with an orthogonal fibre alignment was made from a polyvinyl alcohol (PVA) fibre (1500 denier/300 filaments) which was prepared by gel spinning as an experimental fibre by Unichika Co., Ltd. The fibre had a polymerization degree of 4000 and high strength (17.1 $g d^{-1}$).

A 3-DF, sample no. 9 was produced in the same way as sample no. 8 but from a polyester filament (0.3 mm in diameter).

2.2. Mechanical tests

The following mechanical properties of 3-DFs were measured by an Electric Servo Hydraulic Fatigue Testing Machine (EHF-FD 10KN-10LA, Shimadzu Co., Ltd). They were examined to compare the physical behaviour against loading along or off the direction of fibre alignments as well as to confirm the durability with respect to continuous loading over long periods of time due to the movements in living bodies. The results give the geometric average of three measurements, taken under identical conditions.

2.2.1. Compressive deformation

Strain behaviour with compressive forces along the y- and z-axes in sample nos. 1 and 2 and the z-axis in sample nos. 5, 8 and 9 and the y-axis in sample nos. 6 and 7 were measured. Several kinds of the fabric of no. 11 treated by the below-mentioned surface modification were also measured in comparison.

2.2.2. Tensile deformation

Strain behaviour with tensile forces along the x-axis in sample no. 3 and the x- and y-axes in sample no. 4 were measured. They were examined to compare the mechanical behaviour attributed to non-agreement between loading directions and fibre alignments. The constant deforming rate for all trials was 18 $mm min^{-1}$ at room temperature.

2.2.3. Cyclic bending deformation

Cyclic bending behaviour for up to 10,000 cycles loaded along the z-axis were measured for sample nos. 3 and 4. The bending rate was selected as 2 $mm s^{-1}$ and the distance between the two fulcrums was 90 mm.

2.2.4. Cyclic compressive-tensile deformation

Cyclic compressive-tensile fatigue for up to 100,000 cycles loaded along the z-axis in sample no. 5 and the y-axis in sample nos. 6 and 7 were also measured. The
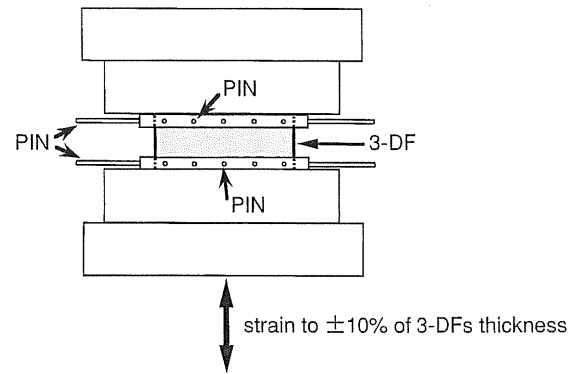

Fig. 1. An example of a securing method for cyclic loading tests.

deformation ratio in all the low cyclic fatigue tests was fixed at 10% of the original length of the axis to be measured. An example of the fixation method for cyclic loading is shown in Fig. 1. Using another method, low cyclic bending fatigues along the z-axis in sample no. 12 were measured for up to 1,000,000 cycles by repeatedly obliquely lifting the lower side up to bend to an angle of 90° in the middle of the fabric body and pulling it down to the initial condition at a rate of 90° per s ($°s^{-1}$). Measurement was taken once the longer arms of the cross-shaped sample no. 12 were returned to their original position.

2.2.5. Cyclic compressing torsional deformation

Compressing torsional fatigues twisted around the z-axis in sample no. 5 and the y-axis in sample nos. 6 and 7 for up to 100 cycles were measured by an Electric Servo Hydraulic Fatigue Testing Machine (EHF-FB10, Shimadzu Co., Ltd). The twist angle and the rate were $\pm 5°$ and $1°s^{-1}$, respectively, and the compressive loading was 200 Newtons (N, i.e. $kg m s^{-2}$).

2.2.6. Creep deformation

The creep deformation in the z-axis in sample no. 5, and the y-axis in sample nos. 6 and 7 was measured under 80 kg loading (i.e. 5.6 $kg cm^{-2}$) at 37°C and 65 RH% for 2400 h (in order to give 10% strain [35] in no. 6) and the residual deformation was measured after 3 days without loading.

2.3. Thermoforming of 3-DF

This experiment was conducted to ascertain how the physical properties changed when a 3-DF was thermoformed to fit a region of the living body in which it is to be implanted. This was because the 3-DF was made of a single long fibre and would disintegrate if the fibre was cut to size. Its change in compressive behaviour along the y-axis was measured (Fig. 8).

The 3-DF sample no. 10, a pseudo-cylindrical shaped off-angle fabric produced from Fibre A was placed into a metal mould having the same concave shape and size as the fabric body and was compressed to the thickness of 14 mm from 16.8 mm by applying pressure from above at 125°C. This temperature, lower than the melting point of UHMWPE (136°C) and higher than that of LLDPE (118°C), was chosen so as to melt the surface of Fibre A and weld the warps, wefts and vertical fibres to each other.

2.4. Transforming into 3-DC

This experimental example was conducted to ascertain how the physical properties changed when a 3-DF was implanted and surrounding tissues entered and filled the textural space as a matrix and consequently forming a 3-DC. Its change in compressive behaviour along the z-axis was measured (Fig. 9).

The 3-DF sample no. 8 was put into a mould having a slightly larger size than the fabric body and an aqueous solution containing about 20 wt% PVA was poured into the mould. This was subjected to freeze–thawing treatment so as to obtain a three-dimensional composite (3-DC) filled and coated with a PVA hydrogel (the fabrication method of which is described in another document [36]) having a cartilage-like hardness.

2.5. Surface modification

The surface of the fibre used in sample no. 11 was oxidized by corona discharge treatment (COROJET® CT-1000 Kyoto Denkiki Co., Ltd) from a distance of 1 cm and for a duration of 5 min so as to alter the contact angle with water. The contact angle was measured by an Origometer (Elma Kogaku Co., Ltd).The corona discharge treatment of a polyethylene surface is widely used in industry to enhance the adhesive properties due to hydrogen bonding between enolizable carbonyls [37]. Thereafter, the LLDPE surface of this 3-DF was softened by heating it to 97°C for 30 min. A micro powder of unsintered hydroxyapatite (u-HA) (Ca/P = 1.69 molecular ratio by chemical analysis) with an average diameter of 2.88 µm (Taihei Chemical Industrial Co., Ltd) was sprayed onto this surface using sandblast apparatus which applied a pressure of 8.5 kgf cm^{-2} through its nozzle head. The u-HA was chosen because of its high bioactivity and total resorbability. It was confirmed by microscopic observation that about 70% or more of the surface area was covered with the powder. After cleaning the surface with water, partial exposure of the powder on the surface was also confirmed. The surface-modified 3-DF plates of sample no. 11 was immersed in simulated body fluid (SBF) [38] at 37°C for 2 weeks.

The crystals which precipitated and covered the surface of the fibre were observed by scanning electron microscopy (SEM) and the chemical composition was analysed by energy dispersive X-ray (EDX). The bonding strength of the HA crystal layer to the LLDPE surface of Fibre A was measured according to the method of JIS ZO237 by peeling with an adhesive tape for industrial use. The immersing test was conducted to ascertain the affinity for the SBF and how and what crystals deposited on the fibre and penetrated into the textural space. The 3-DF after immersion in SBF may be used as an implant material once it has been sterilized, having good surface compatibility and bioactivity if the deposited crystal is a kind of calcium phosphate and can adhere strongly to the surface layer of oxidized LLDPE.

2.6. In vivo tests

The surface modified 3-DF plates made of sample no. 11 treated by the aforementioned corona discharge and then spray-coated with u-HA powder were sterilized with ethylene oxide gas (EOG: EO = 20 wt%, CO_2 = 80 wt%) at 45°C for 5 h. The remaining gas was removed by aeration at 45°C until the gas could no longer be detected by gas chromatography. Then, the plates were implanted in the frontal direction perforating the tibiae and protruding from both the medial and lateral cortices of two male rabbits weighing 3.2 and 3.5 kg, respectively. The operative method was as reported in a previous document [39]. Similarly, the 3-DF plates whose surfaces were not treated at all or only treated with corona discharge were implanted as two controls. The animals were sacrificed 4 and 8 weeks after implantation. The segments of the tibiae containing the fabrics were removed. The segments were prepared for the detaching test by Nakamura's method. The load when the 3-DF broke away from the bone was measured and then the cleaved interface was observed by SEM. The compressive behaviour along the z-axis after in vivo tests were compared with the two controls and the samples immersed in SBF as shown in Fig. 19. These in vivo tests were conducted to ascertain whether the surface-modified 3-DFs were of practical value as implants possessing surface biocompatibility and bioactivity including connectivity with the adjacent cells and tissues, naturally preparing bulk (mechanical) biocompatibility.

3. Results

3.1. Classification of 3-DFs

All the 3-DFs in this article produced by the 3A-3D combination and substantially woven by a single long fibre are shown in Table 1. Although all these 3-DFs could be produced, they were difficult to weave. Sample nos. 1–4 had block-shaped cubic structures. The layers of warps, wefts and vertical fibres in sample nos. 1 and 3

overlap each other with orthogonal alignments. Those of sample nos. 2 and 4 overlap each other with an off-angle alignment where the fibres are intersected obliquely at an angle of 45° in the warps and wefts that are designated as the v- and w-axes as shown by the dotted line.

Similarly, in the semi-elliptic three-dimensional weaves of sample nos. 6 and 7 and in the semi-elliptic and pseudo-cylindrical weave of sample no. 10, the layers of warps and wefts making up the lateral side are crossed with off-angle alignments in which the v- and w-axes are mutually intersected obliquely at an angle of 45° in sample nos. 6 and 10, and at an angle of 30° in no. 7.

Therefore, the mechanical directions to be strained to or from the direction of the x- and y-axes are coincident with the directions of fibre alignments in sample nos. 1, 3, 5, 8, 9 and 11, but are not coincident in sample nos. 2, 4, 6, 7 and 10. The near-net-shaped sample nos. 12 and 13 belong to the complex form that is woven integrally with the combination of orthogonal and off-angle fibre alignments in different parts of the fabric body. The number of warps, wefts, vertical fibres and their layers, and the normal pitch of the planes formed by the x- and y-axes or the v- and w-axes, from which the number of $x\,y$ plane can be calculated, are shown in Table 1. The alignment ratios of the $x:y:z$ or the $v:w:z$ axes are also shown in Table 1.

For example, the block-shaped orthogonal 3-DF sample no. 1 may be described as follows:

size: length × width × height = 24.3 × 24.3 × 24.0 mm
x-axis: 15 fibres × 69 layers
y-axis: 15 fibres × 69 layers
z-axis: (321 × 2) × 19 layers, where '2' means folding alignment ratio of axes (weight ratio or length ratio):

$x:y:z = 1:1:1.$

The block-shaped off-angle 3-DF sample no. 2 may be described by the following:

size: length × width × height = 25.5 × 25.6 × 24.7 mm
v-axis: 22 fibres × 100 layers
w-axis: 22 fibres × 100 layers
z-axis: (144 × 4) fibres × 19 layers where '4' means folding alignment ratio of axes: $v:w:z = 3:3:2.$

The plate-shaped orthogonal fabric sample no. 3 is to an off-angle no. 4 what the block-shaped orthogonal fabric sample no. 1 is to the off-angle no. 2 and similarly, the semi-elliptic fabric sample no. 5 is to sample nos. 6 and 7 that are different in the cross-angle of the layers of warps and wefts making up the lateral v- and w-axes. The 3-DF sample nos. 5–9 and the semi-elliptic and pseudo-cylindrical 3-DF sample no. 10 were fabricated to closely resemble the shape of an intervertebral disc. Sample no. 12 in the cross-shaped form and sample no. 13 in the horseshoe shape were designed with the object of making an artificial finger joint and a meniscus respectively. The real appearances of the 3-DFs in

Table 1 are shown in Fig. 2 and Fig. 3. The textural constructions of an orthogonal fabric and an off-angle ($\pm$45°) fabric are magnified in Fig. 4.

3.2. Physical behaviour

3.2.1. Comparison of compressive behaviour

In the comparison of static compressive behaviour along the y- and z-axes of the orthogonal block fabric sample no. 1 and the off-angle fabric sample no. 2 (Fig. 5), no. 1 showed higher stress at low strain level than no. 2 reaching abo ut 30 MPa at 40% strain. On the contrary, no. 2 showed lower stress even at high strain level (60%) than no. 1 reaching about 15 MPa along the z-axis and only about 5 MPa in the y-axis. All the profiles gave the downward convex 'J'-shaped curve. Consequently, the
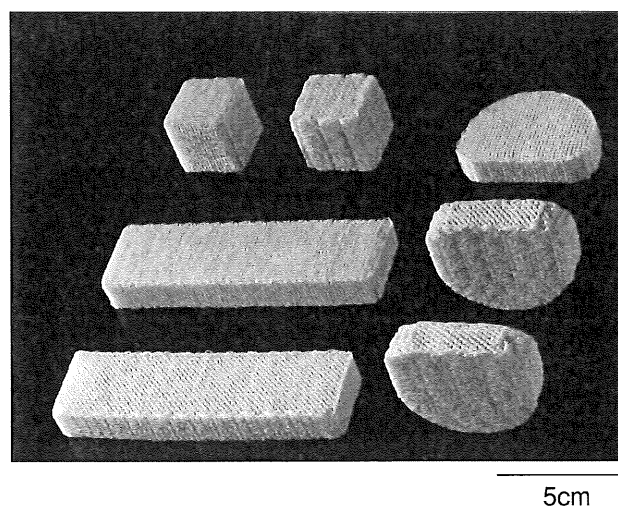

5cm

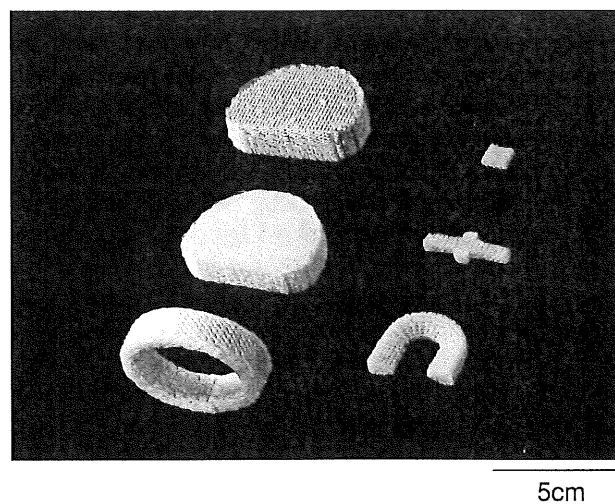Fig. 2. Appearances of 3-DFs (nos. 1–7 in Table 1).
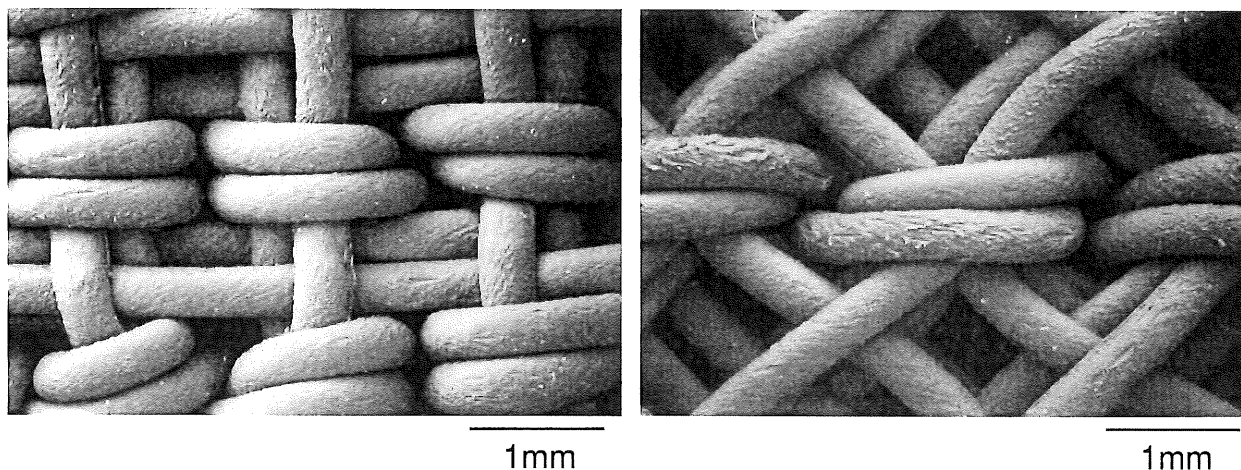

5cm

Fig. 3. Appearances of 3-DFs (nos. 8–13 in Table 1).

Fig. 4. An orthogonal fabric no. 1 (left) and an off-angle (± 45°) fabric no. 2 (right) observed by scanning electron microscope.
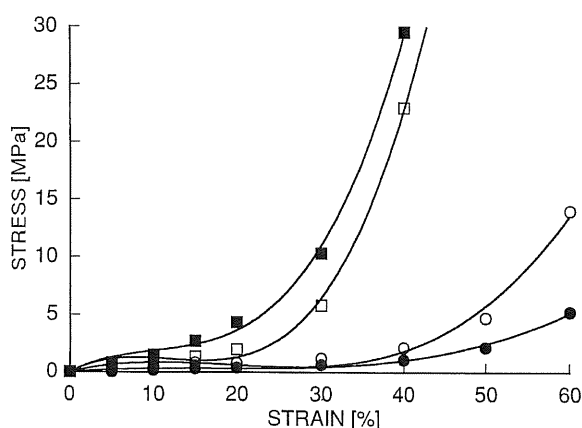

Fig. 5. Compressive behaviour of sample nos. 1 and 2 strained from different axial directions. Orthogonal fabric no. 1 was compressed along the y-axis (■) and the z-axis (□). Off-angle fabric no. 2 was compressed along the y-axis (●) and the z-axis (○).
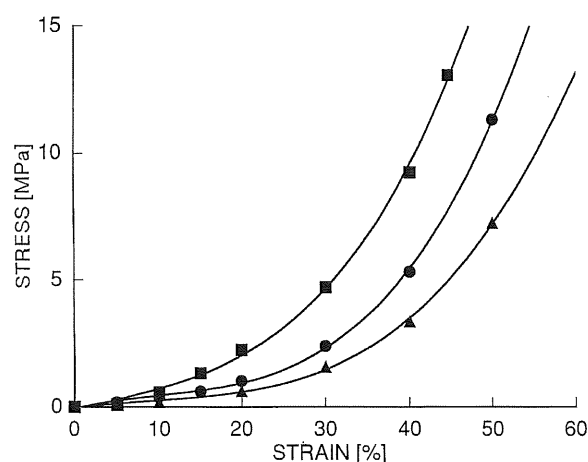
Fig. 6. Comparison of the compressive behaviour of 3-DFs with different cross-angles of fibre alignment strained along the z-axis in orthogonal no. 5 (■); the y-axis in off-angle no. 6 (± 45°) (●); the y-axis in off-angle no. 7 (± 30°) (▲).

off-angle fabric sample no. 2 was shown to be more flexible at low strain level than the orthogonal fabric sample no. 1. Compressive strength in the z-axis of sample no. 2 was higher than that in the y-axis at high strain level. Similarly, in the comparison of compressive behaviour of 3-DFs with different cross-angle of fibre alignments strained from the direction of thickness, that is, along the z-axis in sample no. 5, the y-axis in sample nos. 6 and 7 (Fig. 6), it was clarified that they showed high modulus in accordance to the order of the orthogonal fabric sample no. 5, the off-angle (± 45°) fabric sample no. 6 and the off-angle (± 30°) fabric sample no. 7, although they all gave 'J'-shaped curves.

This order must be mainly attributed to the direction of the external strain force to the fibre alignments. Whether the tangent slope of the 'J'-shaped stress–strain curve increases or decreases depends on the degree of

coarseness or fineness of threads, weave/knit method and textural morphology.

In addition, the quality of the fibre also affected the tangent slope of an S-S curve as shown in Fig. 7, which compares the compressive behaviour of orthogonal 3-DFs made of LLDPE/UHMWPE (no. 5), PVA (no. 6) and polyester fibre (no. 9). 3-DF no. 9 buckled at 10% strain and thereafter gave a 'J'-shaped curve. The buckling at about half the height at an early strain level might be caused by the rigidity of the polyester filament (its diameter was relatively thick at 0.3 mm) and by the lack in flexibility of the textural construction. Sample nos. 5 and 8 both showed almost identical tangent slopes up to the 15% strain level, but thereafter, sample no. 8 gave a steeper slope than that of sample no. 5. This result suggests that Fibre A and the fabric which uses it are more flexible than PVA fibre and its fabric because their
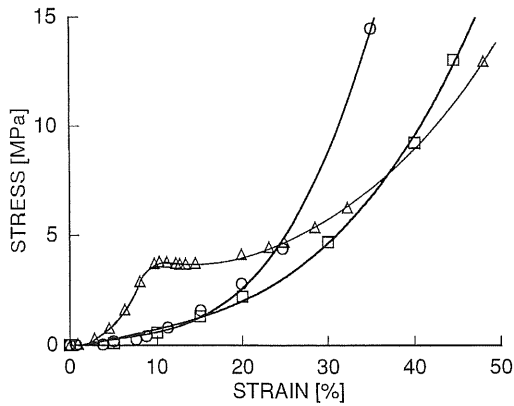
Fig. 7. Comparison of the compressive behaviour of 3-DFs made of different fibres strained along the z-axis: no. 5, LLDPE/UHMWPE (□); no. 8, PVA (○); no. 9, polyester fibre (△).
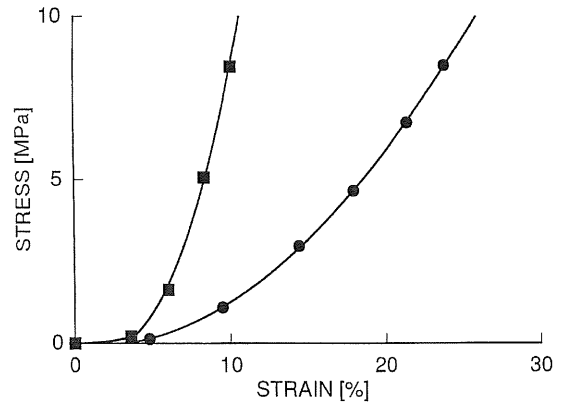

Fig. 9. Change in the compressive behaviour by transforming a 3-DF into a 3-DC. An orthogonal 3-DF created from a PVA fibre (no. 8) (●). A 3-DC transformed by filling the fabric space with PVA gel (■).
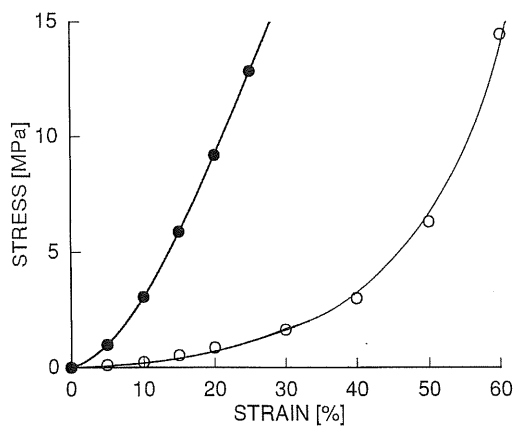

Fig. 8. Change in the compressive behaviour strained along the y-axis by thermoforming a 3-DF: no. 10 (○); thermoformed no. 10 (●).

change into a near 'S'-shaped curve that was relatively rigid at a low strain level. Accordingly, it is necessary to pay attention to the filling mode (matrix ratio, type of material, surrounding tissues, etc.) and morphology when the 3-DF as a matrix type (that is a 3-DC which retains a 'J'-shaped curve) is desired.

3.2.2. Tensile behaviour

The tensile behaviour of the orthogonal plate-shaped fabric sample no. 3 and the off-angle (± 45°) plate-shaped fabric sample no. 4 stretched along the x-axis and the x- and y-axes, respectively, and of the layer 4 of natural adult articular cartilage [40] were compared and the results are shown in Fig. 10.

The tangent slope of sample no. 3 was very steep and the tensile strength was so high that it easily reached 7 MPa at 7% strain. This profile resembled the initial stage of an 'S'-shaped curve. However, examination of the tensile behaviour of sample no. 4 gave a 'J'-shaped curve with a low tangent slope and it barely attained 3 MPa in the direction of the x-axis and 1 MPa at 40% strain of the y-axis. The relatively large tangent slope in sample no. 3 could be attributed to the strength of Fibre A itself stretched in the same direction coincident with the x-axis, and the fairly low slope in sample no. 4 was thought to be due to the deforming strength of the textile structure stretched in the oblique direction against the fibre alignments of the v- and w-axes. As the numbers of layers of the warps and wefts were the same in sample nos. 3 and 4, their profiles in stretching strain were expected to give a similar pattern, but they did not, because of their differences in textural fineness along two axes (x and y). The tangent slope in layer 4 of natural adult articular cartilage parallel to surface cleavage pattern was higher than that of the tensile behaviour of sample no. 4 along the x-axis, but lower than that of sample no. 3 along the x-axis. Accordingly, it is possible

fibre thickness and their arrangement are insignificantly different.

An example of change in compressive behaviour along the y-axis is shown in Fig. 8. The off-angle (± 45°) fabric sample no. 10 was pressurized from above by thermoforming. The tangent slope for sample no. 10 became fairly large by thermo-compressing along its thickness and welding the surface of Fibre A. Also its S-S curve gave nearly the 'S'-shape that is usual in an artificial biomaterial. Since the resulting thermoformed product was harder than its original fabric sample no. 10, it may be used in a part where bone-like hardness is required.

An example of change in compressive behaviour by transforming 3-DF into 3-DC by filling a matrix material among the textural space is shown in Fig. 9. The tangent slope of compressive behaviour along the z-axis in sample no. 8 became steeper by filling the PVA gel as a matrix material and its 'J'-shaped curve tended to

that a 3-DF which is the same as the layer 4 of natural articular cartilage parallel and perpendicular to the surface cleavage pattern can be obtained by increasing the fibre fineness of the v- and w-axes in sample no. 4.

3.2.3. Cyclic hysteresis loss

The hysteresis loss curves of sample nos. 3 and 4 bent along the z-axis are shown in Fig. 11 for comparison. The loading value (Newton) of the orthogonal fabric sample no. 3 reached more than 130 N, but that of the off-angle ($\pm 45°$) fabric sample no. 4 retained only 10 N for the

same stroke (6 mm). The hysteresis loss in sample no. 3 was far greater than that of sample no. 4. This means that sample no. 3 cannot deform easily and requires 130 N to bend up to 6 mm from the initial horizontal level and does not easily recover to the original condition, so that hysteresis loss is fairly large, but sample no. 4 can deform easily and requires only 10 N to bend up to the same distance and easily recover to the original condition, so that hysteresis loss is very small. Fortunately, since both the hysteresis loss curves before and after 10,000 cyclic loadings changed little, sample nos. 3 and 4 can be used as implant materials provided that they are applied to an appropriate region in the living body.

A comparison of the results in the compressive-tensile hysteresis loss curves of 3-DFs with different cross-angles of fibre alignment after 100,000 cyclic loadings is shown in Fig. 12 in contrast with that of a natural intervertebral disc after 4 cyclic loadings which destructed at 4 cycles [41]. The natural intervertebral disc, the orthogonal fabric sample no. 5, the off-angle ($\pm 45°$) fabric sample no. 6 and the off-angle ($\pm 30°$) fabric sample no. 7 gave values of 760 N, 600 N, 480 N and 260 N, at 10% strain, respectively. They gave almost identical hysteresis loss behaviour. The 3-DFs showed little change from the first curves even after 100,000 cyclic loadings. Therefore, these 3-DFs could be expected to be used as artificial intervertebrate discs.

Similarly, a comparison of the results in the compressing torsional hysteresis loss curves of 3-DFs with different cross-angles of fibre alignment after 100 cyclic loadings twisted around the z-axis for sample no. 5 and the y-axis for sample nos. 6 and 7 is shown in Fig. 13 in contrast with that of natural intervertebral disc after 4 cycles under 5 Newtons loading.
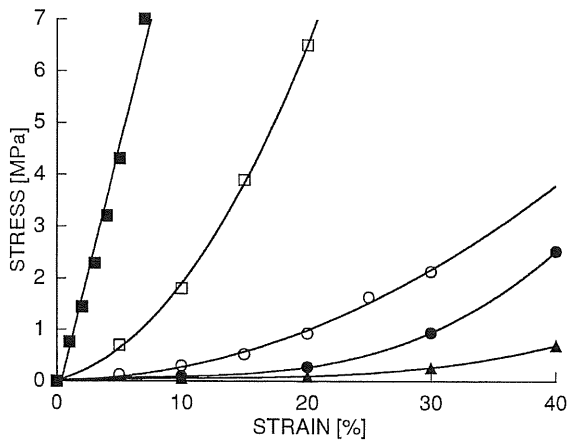

Fig. 10. The tensile behaviour of sample nos. 3 and 4 strained to the different axial directions and natural cartilage to surface cleavage pattern. Orthogonal fabric no. 3 was stretched along the x-axis (■). Off-angle ($\pm 45°$) fabric no. 4 along the x-axis (●) and the y-axis (▲). The layer 4 of natural cartilage, parallel (□) and perpendicular (○) (from Ref. [40]).
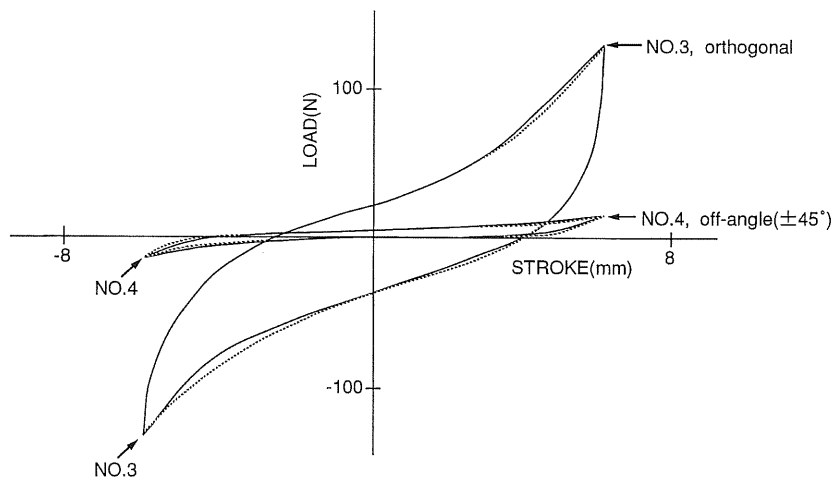

Fig. 11. The hysteresis loss curves of sample nos. 3 and 4 strained along the z-axis by low cyclic bending fatigue. First loading (····) and after 10,000 cyclic loadings (—).
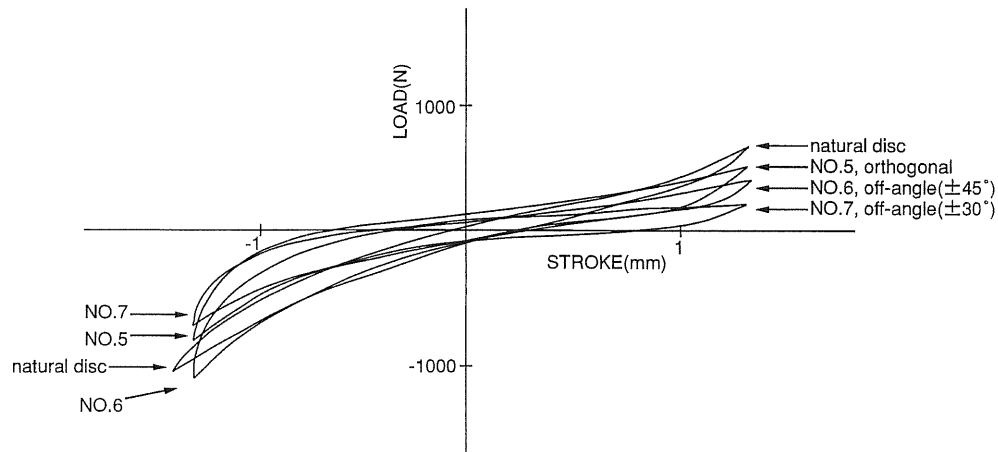
Fig. 12. Comparison of the compressive-tensile fatigue of 3-DFs with different cross-angles of fibre alignment after 100,000 cyclic loadings and natural discs after four cyclic loadings (from Ref. [41]).
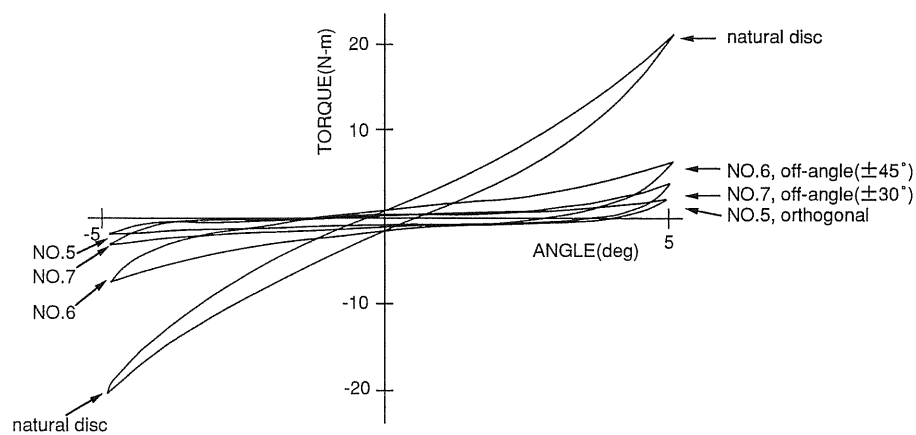

Fig. 13. Comparison of compressive torsional fatigues of 3-DFs with different cross-angles of fibre alignment and natural discs twisted around the z-axis (from Ref. [42]).

The torque value of the natural disc at twist angles of $\pm 5°$ was far higher than those of the three 3-DFs, but this value may have been affected by the torsional strengths of the upper and lower vertebral bodies of the functional spinal units and the material for mounting [41, 42]. Accordingly, the real torque value of the natural disc may be lower than that of the measured one. The torque values for the 3-DFs ranged from the highest for the off-angle ($\pm 45°$) fabric sample no. 6, through the value for the off-angle ($\pm 30°$) fabric sample no. 7, and finally to the lowest for the orthogonal fabric sample no. 5. The hysteresis curves of these 3-DFs showed little variation from the first hysteresis curve even after 100 cyclic loadings. It seemed that the above order for the torque values mainly depended on the cross-angles of the v- and w-axes around the y-axis that was situated as the rotational axis for twist force in sample nos. 6 and 7 and also on the fibre fineness of the fabrics.

The number of warps and wefts making up the lateral v- and w-axes in sample nos. 6 and 7 were as follows:

Sample	Horizontal Axes		Vertical axis
	v-axis fibres × layers	w-axis fibres × layers	z-axis fibres × layers
No. 6	23 × 140	23 × 140	138 × 4
No. 7	17 × 140	17 × 140	119 × 4

This suggests that sample no. 6 showed the highest torque value among these 3-DFs because it had the finest layers of warps and wefts in the v- and w-axes. Since sample no. 7 has a lower cross-angle than that of sample no. 6 because of its high azimuth angle ($\pm 60°$) of fibre alignment around the y-axis, it ought to acquire a higher

torque value provided that sample no. 7 has the same number of fibre as sample no. 6 in the warp and weft layers. Namely, the torque values could range from highest to lowest in the order of sample no. 7, sample no. 6 and sample no. 5 in such a case. Accordingly, it may be necessary to increase the fibre fineness of the v- and w-axes in sample no. 7 or to enlarge the azimuth angle of fibre alignment around the y-axis in sample no. 6 when a higher torque value is required. The degree of hysteresis loss of 3-DFs shown in Fig. 12 and 13 can be regarded as almost identical, so that these improvements in the fibre fineness or the azimuth angle will be effective to some extent. It may be more effective to produce the 3-DFs which have bonding ability to the upper and lower vertebral bodies, when a far higher torque value approximating the functional spinal units (FSUs) which was measured in references 41 and 42 is required.

Fig. 14 shows some hysteresis loss curves for 1,000,000 cyclic bendings to an angle of 90° at the middle of a cross-shaped complex 3-DF sample no. 12 designed with the object of making an artificial finger joint. The initial bending load at 90° was about 2.5 Newtons and the recovering load to the original level (at 0°) was about 4 Newtons. This hysteresis loss curve kept to scores of cycles, but thereafter the values decreased slightly and the hysteresis curves suffered some deterioration, which seemed to be caused from undergoing correction of residual structural strain from when the 3-DF was produced. Bending loads and the hysteresis loss curve did not change significantly and the textile structure remained almost as it was even after 500,000 to 1,000,000 cycles. This result suggests that, with regard to physical properties, sample no. 12 may be used as an implant material.

3.2.4. Creep deformation

The change of creep deformation with time in the 3-DFs strained at 10% of the original thickness in the z-axis direction in sample no. 5 and the y-axis direction in

sample nos. 6 and 7 is shown in Fig. 15. Each strain value for these fabrics was changed to 11, 10, and 14% in turn just after loading and the values were maintained for 2400 h. Their residual strain values were 8, 6, and 9% after 3 days without loading, but recovered to 6, 4, and 5% after 4 weeks without loading. A biomaterial made of a single artificial material or a simple composite and which can retain a constant creep deformation even after 2400 h and then recover fairly close to the original condition after a long period of unloading time is practically unknown. Therefore, these 3-DFs seemed to be suitable for as biomaterial possessing durability for a prolonged period.

3.3. Surface modification

The corona discharged and u-HA powder spray coated surface of sample no. 11 had its contact angle with water altered from 70 to 33°. The resulting contact angle of 33° means an appropriate affinity of 3-DF to the living body fluid [43]. Its surface at 2 weeks after soaking in SBF was analysed by SEM in Fig. 16. It can be observed that u-HA powder was adhered to the LLDPE layer and exposed on the surface (B-1, B-2). HA crystals precipitated onto and covered the surface of Fibre A and entered into its textural space (C-1, C-2) because each value of Ca/P of the precipitated crystals and the sprayed u-HA powder was almost identical 1.65 and 1.72, respectively, calculating from the EDX values (Fig. 17). (The stoichiometric ratio, Ca/P, of HA is 1.67 in theory. These slight differences may be accounted for by analysis methods.) The bonding strength of u-HA crystals with the LLDPE surface of Fibre A was high at over $1.7\,\mathrm{kg\,cm^{-2}}$. This suggested that hydroxyapatite could deposit on and bond strongly to the surface, and the surrounding bone tissues could enter into and mesh with the textural space after only 2 weeks, so that the 3-DFs might have good surface compatibility and bonding
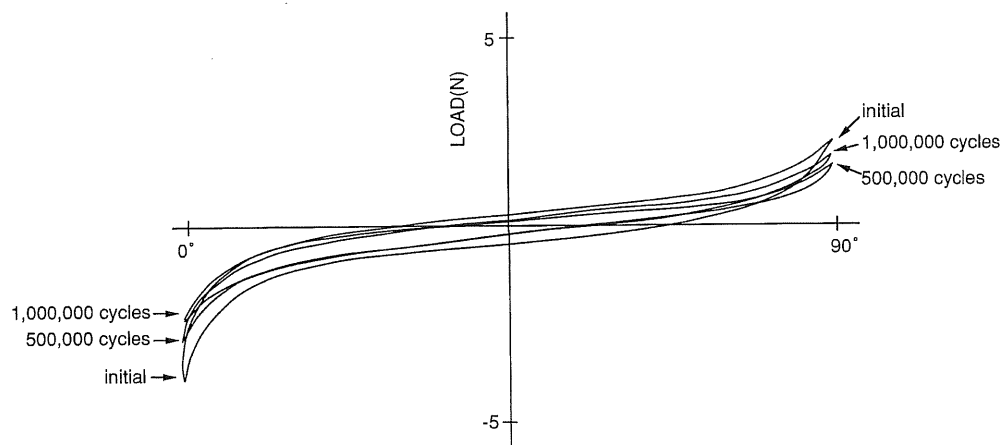

Fig. 14. Hysteresis loss curve for sample no. 12 for up to 1,000,000 cycles of bending to an angle of 90°.
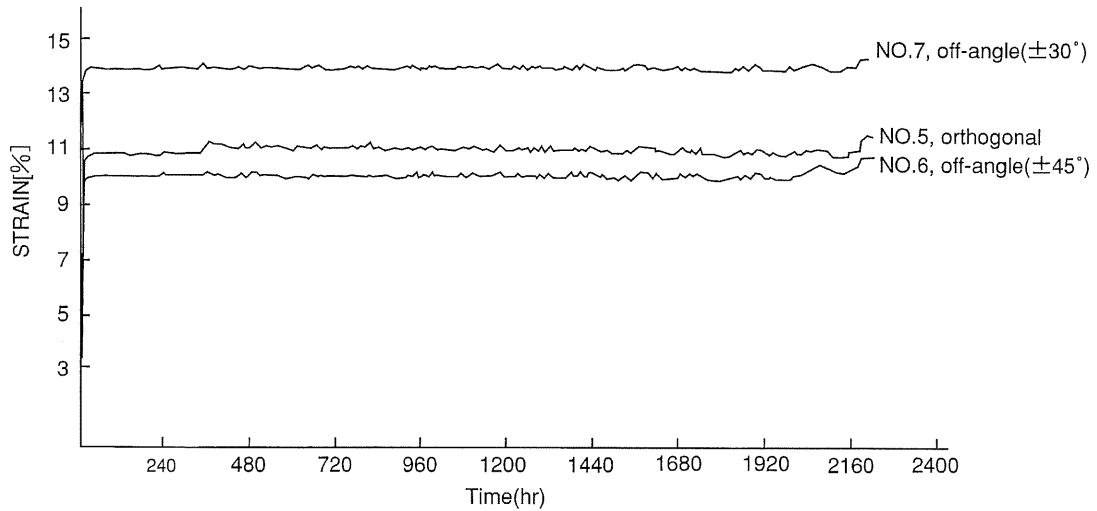
Fig. 15. The change in creep formation with time in 3-DF sample nos 5, 6 and 7 under an 80 kg compressive loading.
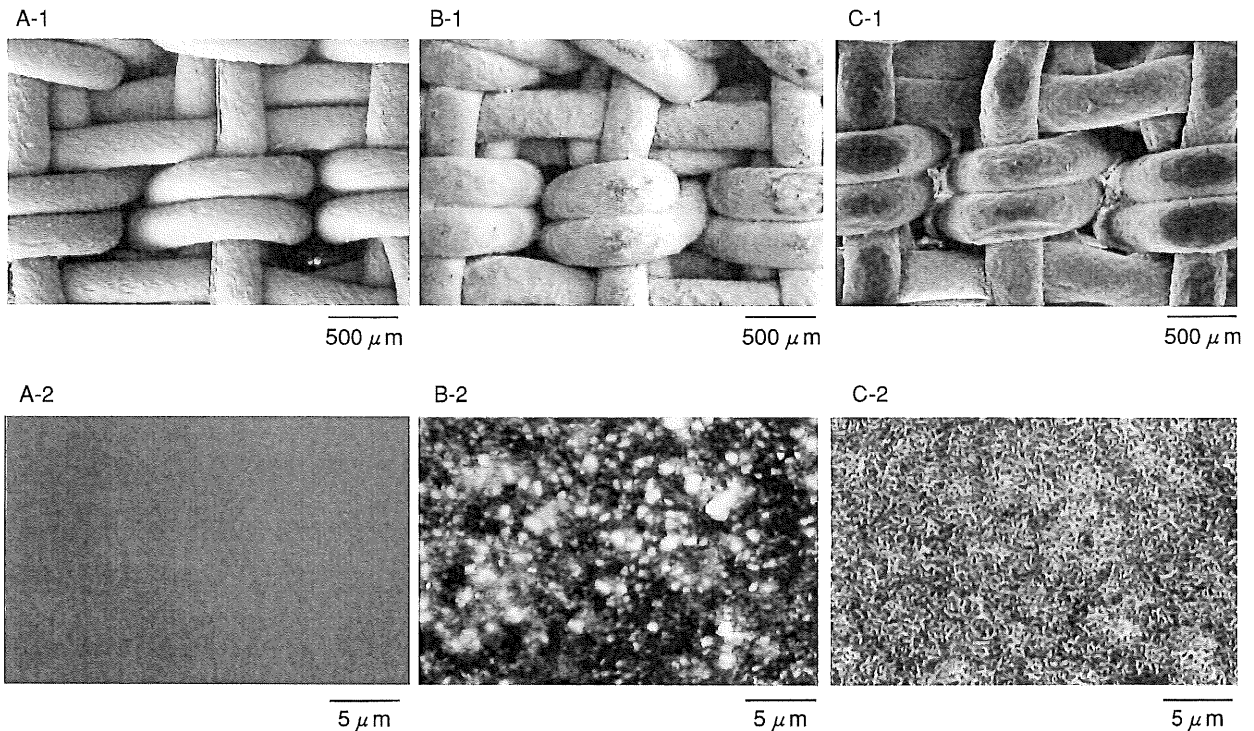

Fig. 16. Surface of sample no. 11 (A-1, A-2). Surface of no. 11 spray-coated with HA powder (B-1, B-2) and after 2 weeks of soaking in simulated body fluid (C-1, C-2).

ability to bone in vivo and are of practical value as biomaterials for implants.

3.4. In vivo tests

Ample surrounding tissues penetrating into the textural space of 3-DF could be observed at 4 weeks (W)

after implantation (Fig. 18A), when a rectangular fabric plate of sample no. 11, the surface of which was modified by treating with corona discharge and spray-coating with u-HA, was implanted in a frontal direction perforating the tibia and protruding from the medial and lateral cortex of a rabbit host. The failure load reached about $1.2 \, kg \, cm^{-2}$ and about $1.7 \, kg \, cm^{-2}$ when the plate

D

E

10 μm
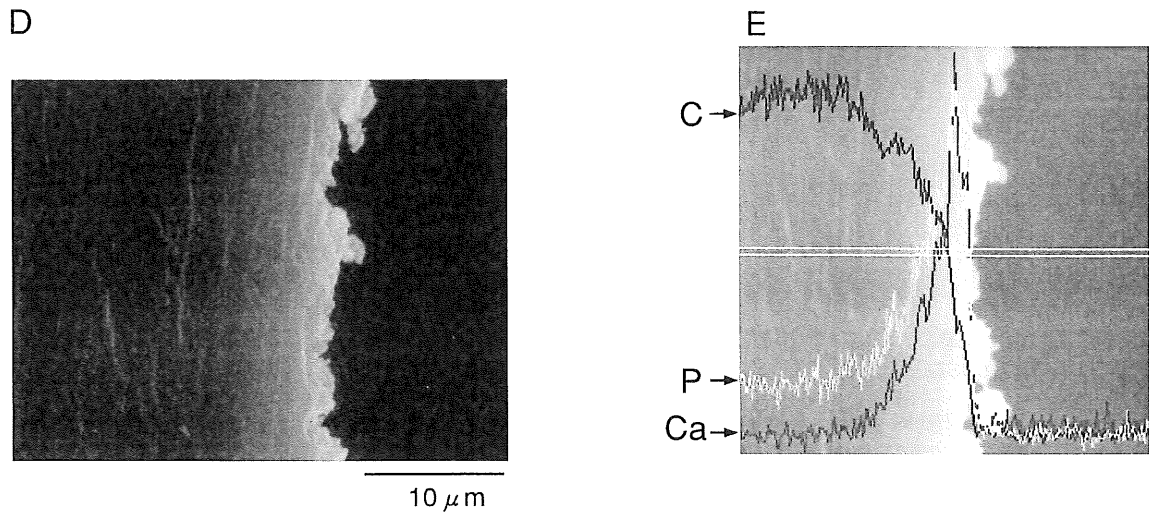
Fig. 17. SEM (D) and EDX (E) of a section of no. 11 spray-coated with HA powder, after 2 weeks of soaking in simulated body fluid.

(A)

(B)

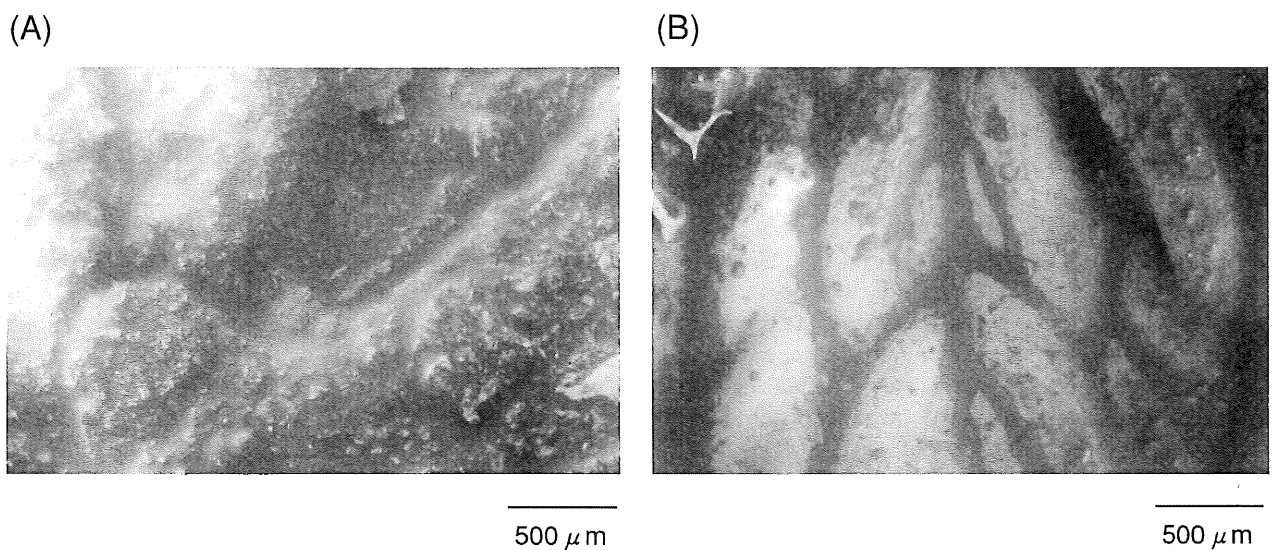500 μm   500 μm

Fig. 18. Surface of 3-DF (surface modified no. 11) after 8 weeks in vivo (A) and its cleaved interfacial layer after a detaching test (B).

detached from the bone at 4 and 8 weeks, respectively. The penetrating tissues were still packing to the full among the textural space when exfoliating the surface tissue layer even after a detaching test (Fig. 18B) and Fibre A did not disconnect with the tissues. On the other hand, in the case of the controls whose surfaces were not treated at all or only treated with corona-discharge, no HA crystal was found on the surface of 3-DF and no tissue meshed among the textural space. This was due to the substantial bioinertness of Fibre A. The period of 8 W for tissue aging was not long enough to harden the osteoblasts, but implantation for longer periods of time may give them hardness similar to natural bone because

the tissue penetrating the textural space at 8 W was harder than that at 4 W, although there is the tissue histology left to be studied.

The compressive stress-strain curves of 3-DF sample no. 11 were steeper for fabrics taken out at 8 weeks after implantation, than those removed after 4 weeks, which were in turn steeper than those removed after 2 weeks after immersion in SBF and the shallowest curves were obtained for two controls in tangent slope although they all gave 'J'-shaped curves (Fig. 19). This order must depend on the degree of filling with deposited crystals or tissues meshed among the textural space. This result could be expected
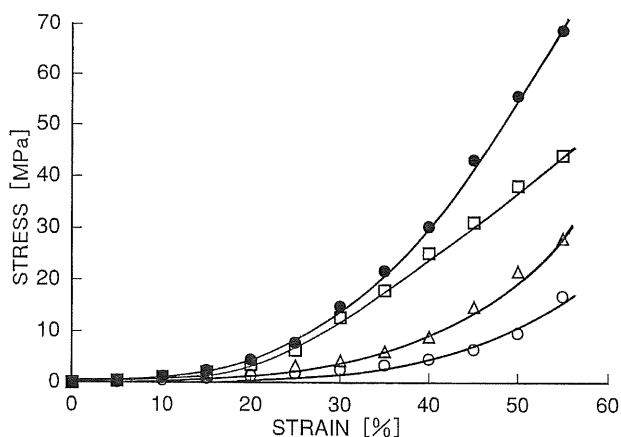
Fig. 19. Comparison of the compressive behaviour of 3-DFs (no. 11) along the z-axis. Control (○); in SBF (2W) (△); in vivo (4W) (□); in vivo (8W) (●).

similarly from the experiment of transforming into 3-DC.

4. Discussion

4.1. Bulk, physical compatibility

The term biomechanical compatibility of materials does not relate to the matching of their absolute strengths [30], but rather to the mutual coincidence of their mechanical behaviour, especially their deformation characteristics. In other words, it means that the stress (strain) respondent to the strain (stress) generated in biological tissues and transferred into an implanted biomaterial is maintained within the normal physiological range of the living body [29].

In general, each artificial material shows an elasticity that corresponds to Hook's law and a linear elasticity (such as viscosity) that corresponds to Newton's law. On the other hand, almost all biological tissues show non-linear elasticity. In other words, artificial materials usually show an 'S'-shaped curve in the stress–strain curve, but biological tissues (especially soft tissues) usually show a 'J'-shaped curve and a loading-unloading cyclic curve having a hysteresis loss. That is, biological tissues generally possess certain properties which cannot be found in conventional artificial materials in that they are pseudo-elastic within a physiological stress range and their stress–strain curves are not equivalent under either loaded or unloaded conditions.

The destruction of a material is divided into 'stress destruction' which is generated when the stress exceeds the strength of the material and 'strain destruction' that occurs when strain by deformation exceeds its limit [44, 45]. Since biological tissues show considerably large deformation before they are destroyed (unlike artificial ma-

terials), the evaluation of materials should be made from the viewpoint of compliance which is the inverse of strength (elastic coefficient) and destruction strain, rather than the strength itself. In particular, in the connecting area of an artificial material with a biological tissue, it is necessary to achieve agreement between the strain and conformity of deformability (flexibility) by matching deformation behaviour rather than matching binding strength.

However, artificial biomaterials have been devised with the idea that physical durability and safety would increase through increasing strength. Such attempts to increase the strength usually results in an increased modulus of elasticity: an 'S'-shaped curve having a larger tangent slope at a small strain. On the other hand, since biological tissues are flexible and strong materials which have high break strength contrary to their low modulus of elasticity (high compliance), namely give a 'J'-shaped curve, it is unavoidable that mechanical incompatibility will exist between conventional biomaterials and biological tissues.

Furthermore, strength and deformation characteristics of a material having a certain form are strongly influenced, not only by its physical properties, but also by its structural factors: design, composition, morphology and so on. Therefore, it seems to be a good idea to effect physical conformity between the natural and artificial materials by simulating the structural factors of biological tissues.

Since the high strength and low modulus of elasticity are contradictory factors in a material made of a single composition and structure, it is necessary to think of a means to satisfy these two factors at once by composing or constructing certain materials. Here is an instructive fact that such biological tissues as articular cartilages, bone matrices, intervertebral discs, ligaments, menisci, nerves, tendons and others contain many collagen fibres arranged in three dimensions.

A product having certain strength and deformation characteristics will be obtained when, as a biomaterial, a woven/knitted fibre structure is constructed so as to resemble those of biological tissues. Since biological tissue has a three-dimensional structure and shows different strength and physical behaviour in each direction, it is necessary to construct a three-dimensional fibre architecture (3-DF) that is made from a single long fibre such as those of the present article, not a laminate structure in which two-dimensional fibre reinforcing plane materials are piled up on top of one another, for there is a danger of delamination between the two-dimensional planes.

Forces such as tensile, compressive, shearing, bending or twisting forces, which will cause breakage and destruction, are always applied to structural cubic bodies from the surrounding biological tissues in the living body at various loading rates continuously and intermittently, statically or dynamically and for short or prolonged

periods of time. Therefore, a 3-DF must have variations which can cope with various loading conditions and match with the mechanical behaviour of its surrounding biological tissues. For medical uses, it should also have the shape (design) variations as shown in Table 1. Such variations of 3-DF can be controlled by altering the weave/knit methods, the thickness and number of fibres in each of the *x*-, *y*- and *z*-axes (degree of packing of filaments in the fabric, and distribution and arrangement conditions), crossing angles of fibre alignment and (for knitted fabrics) the type of fibre knot and tie strength.

All 3-DFs in the present tests showed 'J'-shaped stress–strain curves in the plane comprising the *x*- and *y*-axes and along the *z*-axis. Also, the modulus of elasticity as the tangent slope of the curve could be altered by changing the textural structure of the 3-DF, its fibre material, the degree of packing, the morphology of the matrix and the method of thermoforming. After all, the practicality of durable 3-DFs was supported by the static and dynamic physical behaviour which resembled the compliances of living organisms such as an intervertebral disc, an articular cartilage, menisci, finger joint, or the like.

4.2. Reason for showing 'J'-shaped curves and changing into curves which are nearly 'S' shaped

The following will explain the reason why the 3-DF can show a 'J'-shaped stress–strain curve. Initially, when a slight compressive force is applied from above, the vertical threads loosen slightly between the many knots where the points of interlocking laps are. As the compressive force increases, the strain also increases and the thread distance between each knot becomes shorter and the warps and wefts in planes finally touch each other and the 3-DF becomes a mass of thread compressed in the direction of thickness, so that stress increases exponentially. Finally, the 3-DF shows a large compressive stress as the threads form a mass. As a result, a 'J'-shaped curve is obtained.

On the other hand, the opposite phenomenon occurs when a tensile force is added to the 3-DF. In the initial stage, slightly loosened threads between the many knots are gradually drawn, finally reaching a fully stretched state. Thereafter, the intertwined threads at knotting points are also tied firmly, thus becoming strained. Until this stage, the 3-DF shows a low portion of stress–strain curve. When the tensile force is further increased, resistance caused by the strain increases exponentially, finally reaching the original stress of the threads and, therefore, stopping the extension. As a result, a 'J'-shaped curve is obtained. Similar behaviour can be observed with respect to flexural, torsional and shearing stress.

When a system is created in which a 3-DF is connected with surrounding biological tissues as shown by implantation of the surface modified fabric sample no. 11, it should function in unity with the action of the living body, provided that displacements generated by external forces from the living body are within a range such that the fibres are not damaged or broken but the textural structure is only slightly deformed. In addition, its shape should be maintained to the extent that it is durable even after an extremely large number of repetitions (more than 100,000 or 1,000,000 cycles as shown in Fig. 12 and 14 respectively). However, even in these systems which show 'J'-shaped curves, the 'J' shape may well change to resemble an 'S' shape when it is made into a composite system in which the (biological) material is completely filled among the network space as a matrix [as shown in the system of PVA fiber/PVA gel (Fig. 9) and tests in vivo and in SBF of No. 11 (Fig. 19)], so that it is necessary to pay attention to the filling mode of the 3-DC which is penetrated by surrounding living tissues and to its physical behaviour. Since the degree of non-damage, non-destruction displacement for the 3-DF was also clarified in some experiments to be larger than those by which an ordinary biomaterial made of a solid composition or a usual composite material becomes unrecoverable, the 3-DF may be used as an implant which can unite with the surrounding tissues in physical behaviour.

4.3. Characteristics of fibres and the 3-DFs

When extremely strong ultra-high molecular weight polyethylene (UHMWPE) fibre or similar yarns are used as the fibre of a 3-DF, breakage of the fibre requires extremely high external forces. The strength of the UHMWPE fibre is $35 \, \text{g denier}^{-1}$ in terms of specific strength and $1160 \, \text{g denier}^{-1}$ in terms of specific modulus of elasticity [46], and these values are larger than the respective values of 28 and $1000 \, \text{g denier}^{-1}$ for the Aramid fibre which is considered to be one of the strongest fibres [46]. In consequence, a 3-DF does not break prior to the breakage and destruction of its surrounding biological tissues, so that it has a margin of extremely high safety as a biomaterial from a mechanical point of view.

When surrounding biological tissues penetrate into the fabric space of a 3-DF, fill up the surface and finally cover its outer surface as shown in Fig. 18A, the fabric becomes a part of the native biological tissue as a biomaterial mechanically and physiologically integrated with the biological tissue. Therefore, a completely substituted state with surrounding living tissues can be obtained in the case of 3-DF made of totally degradable and absorbable fibres such as of polyglycolide, polylactide or polydioxanone, although excess polymer debris may cause an intermittent foreign body reaction in the processes of degradation and absorption and its strength is considerably lower than that of UHMWPE [47, 48].

Thus, it was confirmed that 3-DF is a biomaterial which satisfies bulk compatibility wherein mechanical compatibility are taken into consideration. Note that even in the case of an implant material which has bulk compatibility, each fibre must have surface compatibility as its composing unit.

The following is a discussion of fibres. Examples of fibres used so far as trial and practical biomaterials include synthetic fibres such as nylon, polyethylene terephthalate, polypropylene, polyethylene (ultra-high molecular weight) and polyurethane; natural fibres such as silk, collagen, chitin and chitosan; and biologically degradable and absorbable fibres such as polyglycolide, polylactide, glycolide-lactide copolymer and polydioxanone. In addition to these fibres, hydrophilic fibres such as polyvinyl alcohol have been studied. As a matter of course, for medical purposes it is possible to use these fibres alone or as blended yarns in the 3-DF form.

Inorganic fibres such as carbon fibre and hydroxyapatite fibre may also be used, but are not desirable materials because of their rigid and fragile properties which result in technical difficulties when making the 3-DF structure and a tendency to form much debris due to the breakage of fibres at the time of weaving, as well as the possibility of generating a foreign body reaction after implantation in the living body due to the formation and release of fibre debris. Consequently, it is desirable to select a base material for a 3-DF carefully, even in a matrix system with organic polymers or ceramics.

Fibres are divided into staples and filaments and, in either case, they are used as one yarn unit for weaving as they are or, when a thread is too thin, after tying up several threads in a bundle or twisting them to make a thick yarn. However, there is a limit in desirable thickness, because apparent rigidity becomes high when the yarn is too thick, thus making the weaving difficult. Therefore, thin threads are used by tying them up in a bundle in most cases. However, when the staple-composing thread unit is too thin, the threads become loose and cause a disadvantageous hairiness at the time of the three-dimensional fabric processing and during a prolonged period of stressed time in the living body. In such cases, the deterioration of physical properties and irritation of the surrounding tissues are probable. Accordingly, filaments having an appropriate thickness are more desirable.

The aforementioned organic fibres can be classified into the following types:

(i) bioinert fibres such as polyethylene and polypropylene;

(ii) bioaffinitive fibres such as polyurethane, polyvinyl alcohol and silk; and

(iii) biocompatible and biologically degradable and absorbable fibres such as collagen, chitin, chitosan, polyglycolide, polylactide, glycolide/lactide copolymers and polydioxanone.

Since the fibres belonging to group (i) are biologically inert, they are useful for an implant material which will be in the living body for a prolonged period of time. On the other hand, the fibres of group (ii) have bioaffinity but no decisive proof of not causing critical damage by a foreign body reaction when implanted for a prolonged period of time, so that it is necessary in some cases to reoperate for removal when the objective has been achieved. Since the fibres of group (iii) are eventually degraded and absorbed, they can be used as a scaffold where regeneration of the biological tissue is possible [49–51].

These fibres can be used properly according to their characteristics, although (i), (ii) and (iii) have no bioactivity. Therefore, it is absolutely necessary to produce fibres (iv) which can provide a chance for and an area of connectivity with tissues, namely fibres to which bioactivity (tissue connectivity) is endowed by physically and chemically modifying the surface of the fibres of (i), (ii) or (iii).

A 3-DF made of fibres of group (iv) that are modified on the surface of the fibre of group (i) is desired for an implant material to be present for a prolonged period of time in the living body. A surgical suture is used in small amounts and does not require long-term durability. However, whether a 3-DF has biologically inert or active biocompatibility is an essential factor in avoiding foreign body reaction when it is used for the purpose of the filling, prothesis, substitution, reconstruction and other such treatments of damaged regions of a living body where various cubic shapes, respective volume and long-term durability (no deterioration) or tissue conductivity, inductivity and connectivity are required. Long-term durability means that there is no chemical or physical (mechanical) deterioration.

Although attempts have been made to use some synthetic fibres, which have higher strength than biological tissues, as implants, they are not suitable for long-term implantation because of their insufficient biocompatibility and insufficient mechanical durability due to deterioration in the living body. An excellent implant material which has suitable mechanical properties, long-term durability and biocompatibility together must be obtained by the use of a three-dimensional structure of inert synthetic fibres, especially those having high strength that can withstand extreme loads unexpectedly applied to the living body and having a modified surface to give biological activity as shown in this article. In this case, tissues around the implant gradually penetrate into the textural space of the three-dimensionally intertwined fibres. Not only chemical bonding but also strong physical bonding due to an anchoring effect can be obtained. Under certain circumstances, the surrounding tissues cover up the 3-DF and they can adapt themselves to the movement of surrounding tissues. The structural morphology of the 3-DF is effective for the induction of

shapes and synchronization of mechanical strain with the surrounding tissue.

4.4. Surface modification and its effect

Surface modification can be effected by various means such as chemical methods, physical methods, and combinations thereof which are described in detail in other documents [52–56]. When classified from the view point of plastic surface treatment methods, they are divided into (A) dry treatment and (B) wet treatment. Treatment (A) includes discharge treatment (corona discharge and glow discharge), flame treatment, ozone treatment, ionized ray treatment (ultraviolet ray, radiation, and electron beam), rough surface treatment, polymer blend (different polymer and filling of inorganic substance, and (B) includes chemical agent treatment, primer treatment, polymer coating, electro-decomposition and catalyst-aided graft.

Since bioactive inorganic bioglass, apatite wollastonite glass ceramics (AW-GC), hydroxyapatite (HA), α-, β-tricalcium phosphate (α-TCP, β-TCP), tetracalcium phosphate (TeCP), octacalcium phosphate (OCP) are available as materials for hard tissue inclusive of every cartilage in the field of orthopaedic surgery, a material capable of bonding to the living body can be produced effectively in which these bioactive materials are sprayed onto the fibre surface which is slightly softened by heating, with a portion of the powder particles being exposed on the surface as shown in Fig. 16B. As an alternative method, a material capable of inducing bone tissue can be produced by introducing phosphate groups to the surface of a polymer [57]. A method in which a natural biomaterial such as collagen, gelatin, fibronectin, hyaluronic acid or heparin is fixed on the material surface making use of the aforementioned surface treatment methods is one of the most effective methods for the purpose of producing a material which can combine sufficiently with soft tissues such as connective tissues.

5. Conclusion

The 3-DFs of organic polymeric fibres having the aforementioned surface characteristics, especially those that have been treated with corona discharge and bioceramics powder, have good surface bioactivity and bulk biocompatibility so that they can be used as biomaterials which have sufficient tissue connectivity and mechanical durability to withstand long-term implantation. At present, several animal tests are being undertaken to devise such implants as novel and effective artificial articular cartilages, intervertebral discs and menisci, materials for osteosynthesis and prosthesis, and the like. The 3-DFs

evaluated in this article were limited to triaxial three-dimensional (3A-3D) fabrics, but more complex shaped 3-DFs with multi axial three-dimensional (mA-3D, $m > 4$) development can also be created and used as biomaterials for implants.

Acknowledgements

References

[1] Frank KKO. Preform fiber architecture for ceramic-matrix composites. Ceramic Bull 1989;68(2):401–14.

[2] Bailie JA. Woven composite structures, In: Lee SM, editor. International encyclopedia of composites, vol. 6. New York: VCH Publishers, 1990:110–122.

[3] Yang JM. Processing and performance of braided composites. In: Lee SM, editor. International encyclopedia of composites, vol. 4. NewYork: VCH Publishers, 1990:449–63.

[4] Ngai TT. Carbon–carbon composites. Lee SM, editor. International encyclopedia of composites, vol. 1. New York: VCH Publishers, 1990:158–87.

[5] Bruno PS, Keith DO, Vicario AA. Automatically woven three-directional composite structures. Soc Adv Mat Process Engng Q 1986;7(4):10–17.

[6] Rolincik PG. Autoweave™—a unique automated 3-D weaving technology. Soc Adv Mater Process Engng J 1986;23(5):40–47.

[7] Popper P, Braiding. In: Lee SM, editor. International encyclopedia of composites, vol. 1. New York: VCH Publishers, 1990:130–47.

[8] Rushton N, Ali MS, Hastings GW, Rae T, Ross ERS, Wynn-Jones CH. Carbon fiber composite bone plates-development, biological testing and early clinical experience. J Bone Joint Surg Brit Vol 1990;72B:586–91.

[9] Tayton K, Johnson-Nurse C, McKibbin B, Bradley JS, Hasting GW. The use of semi-rigid carbon-fibre-reinforced plastic plates for fixation of human fractures. Results of preliminary trials. J Bone Joint Surg Brit Vol 1982;64B:105–11.

[10] Mayer J, Ruffieux K, Koch B, Wintermantel E, Schulten T, Hatebur A. The Double Die Technique (DDT): biomaterials processing for adaptable high fatigue resistance thermoplastic-carbon fiber ostheosynthesis plates. Biomed Engng App 1993;5:778–83.

[11] Ruffieux K, Hintermann M, Mayer J, Wintermantel E. Enhanced local carbon fiber knitting reinforcement of isoelastic bone plates. Concept of a new implant. In: Textiles and Composites '92. VTT Technical Research Center of Finland, Espoo, 1992:326–32.

[12] Mayer J, Ruffieux K, Ha S, Koch B. Knitted carbon fiber reinforced biocompatible thermoplastics: influence of structural parameters on manufacturing techniques and mechanical properties. In: Proc. Int. Symp. Adv. Materials Lightweight Structures. ESTEC, Nortwijk, NL, 1994:351–58.

[13] Mayer J. Gestricke aus Kohlenstoffasern für Biocompatible Verbund Werkstoffe, dargestellt an einer homoelastischen osteosyntheseplatte. Dissertation, ETH Zürich, 1994.

[14] Mayer J, Ruffieux K, Tognini R, Wintermantel E. Knitted carbon fibers, a sophisticated textile reinforcement that offers new perspectives in thermoplastic composite processing, In: Bunsell AR, Kelly A, Massiah A, editors. Developments in the science and

technology of composite materials. Abington, Cambridge, UK: Woodhead Publishing Ltd., 1994:219–24.

[15] Hastings GW. Is there an ideal implant for fracture fixation? Symposium on biodegradable implants in fracture fixation. The International Society for Fracture Repair 1993:7–8.

[16] Mayer J, Ha SW, De Haan J, Petitmermet M, Wintermantel E. Knitted carbon fiber reinforced biocompatible thermoplastics, mechanical properties and structure modeling. In: Bunsell AR, Kelly A, Massiah A, editors. Developments in the science and technology of composite materials, Abington: Woodhead Publishing Ltd., 1993:637–42.

[17] Mayer J, Giorgetta S, Koch B, Wintermantel E, Padscheider J, Spescha G. Characterization of thermal oxidized carbon fiber surfaces by ESCA, wetting techniques and scanning probe microscopy and the interaction with polyethylmethacrylate. Development of a biocompatible composite material. Composites 1994;25:763–69.

[18] Ko FK. Prefome fiber architecture for ceramic-matrix composites. Ceram Bull 1989;2:401–14.

[19] Ko FK, Whyte DW, Pastore CM. Control of fiber architecture for tough net-shaped structural composites, In: Proc. of MiCon 86, Optimization of processing, properties and service performance through microstructural control. ASTM Special Technical Publication 979, ASTM, Philadelphia 1986:291–98.

[20] Fukuta K, Onooka R, Aoki E, Nagatsuka Y. Application of latticed-structure composite materials with three dimensional fabrics to artificial. Bull Res Inst Polym Text 1982;131:151–59.

[21] Noishiki Y, Watanabe K, Okamoto M, Kikuchi Y, Mori Y. Evaluation of a new vascular graft prosthesis fabricated from ultra fine polyester fiber. ASAIO Trans 1986;32:309–14.

[22] King MW. Designing fabrics for blood vessel replacement. Can Text J 1991;108(4):24–30.

[23] King MW, Guidoin RG, Gunasekera KR, Gosselin C. Designing polyester vascular prostheses for the future. Med Prog Tech 1983;9:217–26.

[24] Duncan E. DuPont issues materials policy. Biomater Forum 1993;15(2):1–17.

[25] Fujukawa K. Clinical study on anterior cruciate reconstruction with the Leeds-Keioartificial ligament. In: Prosthetic ligament reconstrued. London: W.B. Saunders Co., 1988:132–39.

[26] McPherson GK, Mendenhall HV, Gibbons DF, Plenk H, Rottmann W, Sanford JB, Kennedy JC, Roth JH. Experimental mechanical and histologic evaluation of the Kennedy ligament augmentation device. In: Prosthetic ligament reconstrued. Clin Orthop 1985;196:186–95.

[27] Scharling M. Replacement of the anterior cruciate ligament with a polyethylene prosthetic ligament. Acta Orthop Scand 1981;52:575–78.

[28] Ikada Y. Interfacial biocompatibility. In: Shalaby SW, Ikada Y, Langer R, Williams J, editors. Polymers of biological and biomedical significance. ACS Symposium Series 540. Washington, 1994:35–48.

[29] Williams DF. Definitions in biomaterials In: Progress in biomaterial engineering. Amsterdam: Elsevier, 1987, vol. 4.

[30] Williams DF. Biofunctionality and biocompatibility. In: Williams D, editor. Materials science and technology. Medical and Dental Materials. New York: VCH Publishers, 1992;14:1–27.

[31] Tsutsumi S. Biomechanics for implant. J Jap Soc for Biomater 1991;9(4):200–11 (in Japanese).

[32] Ikada Y. Surface modification of polymers for medical applications. Biomaterials 1994;15(10):725–36.

[33] Dow NF, Tranfield G. Preliminary investigation of feasibility of weaving triaxial fabrics (Dow Weave). Tex Res J 1970; 40(11):986–98.

[34] Hirokawa T. JP 1565997 (in Japanese).

[35] Vuono-Hawkins M, Langrana NA, Parsons JR, Lee CK, Zimmerman MC. Materials and design concepts for an intervertebral

disc spacer. II. Multidurometer composite design. J Appl Biomater 1995;6:117–23.

[36] Noguch T, Yamamuro T, Oka M, Kumar P, Kotoura Y, Hyon SH, Ikada Y. Poly(vinyl alcohol) hydrogel as an artificial articular cartilage: evaluation of biocompatibility. J Appl Biomater 1991;2:101–07.

[37] Blythe AR, Briggs D, Kendall CR, Rance DG, Zichy VJI. Surface modification of polyethylene by electrical discharge treatment and the mechanism of autoadhesion. Polymer 1978; 19(11): 1273–78.

[38] Kokubo T, Ito S, Huang ZT, Hayashi T, Sakka S, Kitsugi T, Amamuro T. Ca, P-rich layer formed on high-strength bioactive glass-ceramic A-W. J Biomed Mater Res 1990;24:331–43.

[39] Nakamura T, Yamamuro T, Higashi S. A new glass-ceramic for bone replacement: Evaluation of its bonding to bone tissue. J Biomed Mater Res 1985;19:71–84.

[40] Kempson GE. Mechanical Properties of articular cartilage. Adult Articular Cartilage 1979:333–414.

[41] Asano S, Kaneda K, Umehara S. Tadano S. The mechanical properties of the human L4-5 functional spinal unit during cyclic loading. Spine 1992;17(11):1343–52.

[42] Tadano S, Ishikawa H, Asano S, Kaneda K. Structural design of an artificial intervertebral disc. Proceedings of Annual Meeting of Japanese Society for Orthopedic Biomechanics 1991;13:75–79 (in Japanese).

[43] Ikada Y. Blood-compatible polymers. In: Fendler JH, editor. Membranes mimetic approach to advanced materials. Advances in polymer science 57, Berlin, Heidelberg: Springer-Verlag, 1984:103–40.

[44] Fung YC. Biomechanics. Mechanical properties of living tissues. Berlin, Heidelberg: Springer-Verlag, 1981:133–42.

[45] Fung, YC, Hayashi K, Seguchi Y. Progress and new directions of biomechanics. Mita Press, 1989:433–42.

[46] From a brochure UHMWPE TEKMILON®. (Misui Petrochemical Co. Ltd.) (in Japanese).

[47] Scherer MA, Früh HJ, Ascherl R, Mau H, Siebels W, Blümel G. Kinetics of resorption of different suture materials depending on the implantation site and species. In: Planck H, Dauner M, Renardy M, editors. Degradation phenomena on polymeric biomaterials. Berlin, Heidelberg: Springer-Verlag, 1992:77–96.

[48] Gibbon DF. Tissue response to resorbable synthetic polymers. In: Planck H, Dauner M, Renardy M, editors. Degradation phenomena on polymeric biomaterials. Berlin, Heidelberg: Springer-Verlag, 1992:97–104.

[49] Mooney DJ, Mazzoni CL, Breuer C, McNamara K, Hern D, Vacanti JP, Langer R. Stabilized polyglycolic acid fiber based tubes for tissue engineering. Biomaterials 1996;17(2):115–24.

[50] Mikos AG, Bao Y, Cima LG, Ingber DE, Vacanti JP, Langer R. Preparation of poly(glicolic acid) bonded fiber structures for cell attachment and transplantation. J Biomed Mater Res 1993;27:183–89.

[51] Vacanti JP, Vacanti CA, Langer RS. USP. 5041138.

[52] Muster D, Demri B, Hage AM. Physicochemical characterization of surface and interface on biomaterials and coatings. In: Trantolo W, Yazemski A, Schwartz G, editors. Encyclopedic handbook of biomaterials and bioengineering. Part A: Materials, vol. 1. New York: Dekker, 1995:785–812.

[53] Chehroudi B, Brunette DM. Effects of surface topography on cell behavior: In: Trantolo W, Yazemski A, Schwartz G, editors. Encyclopedic handbook of biomaterials and bioengineering. Part A: Materials, vol. 1. New York: Dekker, 1995:813–42.

[54] Olivieri MP. Interfacial biophysics; relating structure to function at surfaces. In: Trantolo W, Yazemski A, Schwartz G, editors. Encyclopedic handbook of biomaterials and bioengineering. Part A: Materials, vol. 1. New York: Dekker, 1995:843–64.

[55] Sheu MS, Hudson DM, Loh IH. Biomaterials surface modification using plasma gas discharge processes. In: Trantolo W,

Yazemski A, Schwartz G, editors. Encyclopedic handbook of biomaterials and bioengineering. Part A: Materials, vol. 1. New York: Dekker, 1995:865–94.

[56] Aoms RA, Anderson AB, Clapper DL, Duquette PH, Duran LW, Hohle SC, Sogard DJ, Swanson MJ, Guire PE. Biomaterials surface modification using photochemical coupling technology.

In: Trantolo W, Yazemski A, Schwartz G, editors. Encyclopedic handbook of biomaterials and bioengineering. Part A: Materials, vol. 1. New York: Dekker, 1995:895–926.

[57] Tretinnikov ON, Kato K, Ikada Y. In vitro hydroxyapatite deposition on to a film surface-grafted with organophosphate polymer. J Biomed Mater Res 1994;28:1365–73.